

ABSTRACT

The paper describes the model for the calculation of stress-strain distribution in composite material rotors. Composite rotors can be calculated with this model using the finite element method. The predicted data from these calculations has been compared with measured data.

The influence of applying pretension to the composite during manufacturing, has been studied as well as the influence of temperature and shrinkage on the stress-strain distribution within the rotors.

STRESS CALCULATION

Stress calculation is based on four different loads, the rotational load, pretension load, thermal load and shrinking. These loads are modeled and calculated using finite element method.

STRESS AND STRAIN DUE TO ROTATION

The centrifugal load (F) acting on a thin rim with the thickness Δr is found to be

$$F = 2\pi * \rho r^2 \Delta r h * \omega^2 \quad (1.)$$

ρ : density of the composite material

r : radius of the ring

h : thickness of the rotor

ω : angular velocity

The stress distribution of thin, axis-symmetric disks is only dependent on the radius (r) and not on the thickness of the rotor (h). Therefore it is possible to write the condition of equilibrium for the stress distribution as shown in equation (2.)

$$\begin{aligned} \frac{\partial}{\partial r} \sigma_{\perp} r h - \sigma_{\parallel} h + \rho \omega^2 r^2 h &= 0 \\ \frac{\partial}{\partial r} \tau_{\perp \parallel} r h + \tau_{\perp \parallel} h - \rho \frac{\partial}{\partial t} \omega r^2 h &= 0 \end{aligned} \quad (2.)$$

σ : strain \perp : normal to the fibre
 τ : shear \parallel : parallel to the fibre

And the condition of strain equilibrium is:

$$\varepsilon_{\perp} = \frac{\partial}{\partial r} (\varepsilon_{\parallel} * r) \quad (3.)$$

Together with the material properties the following differential equation for the strains in radial and tangential direction can be found and implemented in the finite element model:

$$\begin{aligned} \frac{\partial^2}{\partial r^2} \sigma_{\perp} + \frac{\partial}{\partial r} \sigma_{\perp} \left(\frac{3}{r} + \frac{1}{h} \frac{\partial h}{\partial r} \right) + \\ + \sigma_{\perp} \frac{1}{r^2} \left((1 - \mu^2) + r(2 + \nu_{\parallel \perp}) \frac{1}{h} \frac{\partial h}{\partial r} + r^2 \frac{\partial h}{\partial r} \left(\frac{1}{h} \frac{\partial h}{\partial r} \right) \right) + \\ + \rho \omega^2 (3 - \nu_{\parallel \perp}) = 0 \end{aligned} \quad (4.)$$

tangential stress

$$\sigma_{\parallel} = \frac{\partial}{\partial r} (\sigma_{\perp} * r) \quad (5.)$$

STRESS AND STRAIN DUE TO PRETENSION

The manufacturing process, developed by the Swiss Federal Institute of Technology (Widmer, 1985), makes it possible to apply a circumferential preload to the composite. This method allows the controlled optimization of the stress-strain distribution within the composite material rotor.

Figure 1 shows a sketch of the woven ribbon winding method. The maximum applicable pretension is currently 10'000N.

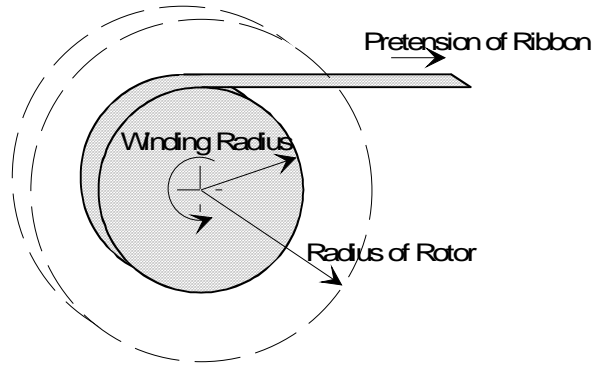


Figure 1: Manufacturing Process for High Speed Rotors

Pretension applied to the ribbon, results in a tension of the fibre ribbon and in a radial prestress keeping the inner layers under stress.

Figure 2 shows the nomenclature for the calculation of the prestress:

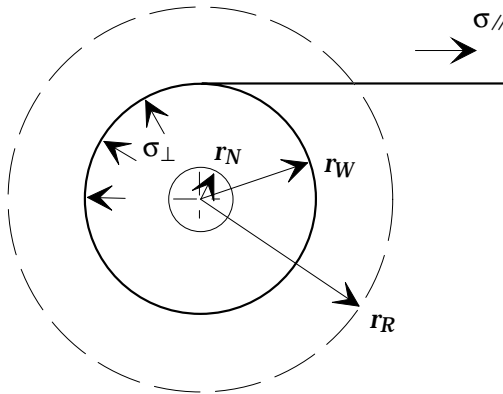


Figure 2: Pretension Applied to a Rotor

At a given pretension, the radial pressure beneath the actual winding diameter can be calculated with:

$$\sigma_{\perp}(r_w) = \sigma_{\parallel}(r_w) * \frac{d_B}{r_w} \quad (6.)$$

This radial pretension only has an effect on the rotor at a radius (r) smaller than (r_w). Therefore it is necessary to integrate all local radial stresses over the whole radius of the rotor to obtain the stress distribution in the rotor due to pretension. The stress distribution implemented in the model can be obtained from (6.) and (4.).

THERMAL LOAD

Thermal load can influence the stress-strain distribution of a rotor in two ways. First is it possible that the curing temperature causes remarkable stresses in the composite if the rotor has been cured at elevated temperatures. In some cases the normal operation temperature should not be neglected. Thermal load results in the following thermal stress with the thermal expansion coefficient (α), the Young's modulus (E) and the rotor temperature (T):

$$\begin{aligned} \sigma_{\parallel}(1 + \nu_{\perp\parallel}) - \sigma_{\perp}\left(\frac{E_{\parallel}}{E_{\perp}} + \nu_{\parallel\perp}\right) + r\left(\frac{\partial}{\partial r}\sigma_{\parallel}\right) \\ - r\nu_{\parallel\perp}\left(\frac{\partial}{\partial r}\sigma_{\perp}\right) - TE_{\parallel}(\alpha_{\perp} - \alpha_{\parallel}) = 0 \end{aligned} \quad (7.)$$

Thermal stress can be remarkably large, depending on the curing temperature and the size of the rotor, so that a failure of the rotor without rotational load is possible.

SHRINKING LOAD

As matrix for the composite material epoxy resins are commonly used. The shrinking of epoxy-resins during the manufacturing process is in the order of 5%. This causes radial and tangential strains according to the following formulae:

$$\begin{aligned} \epsilon_{\parallel} &= \frac{E_M}{E_{\parallel}} * \epsilon_{M_s} \\ \epsilon_{\perp} &= \frac{E_M}{E_{\perp}} * \epsilon_{M_s} \end{aligned} \quad (8.)$$

A typical radial stress distribution, with different loads as discussed above are shown in Figure 3:

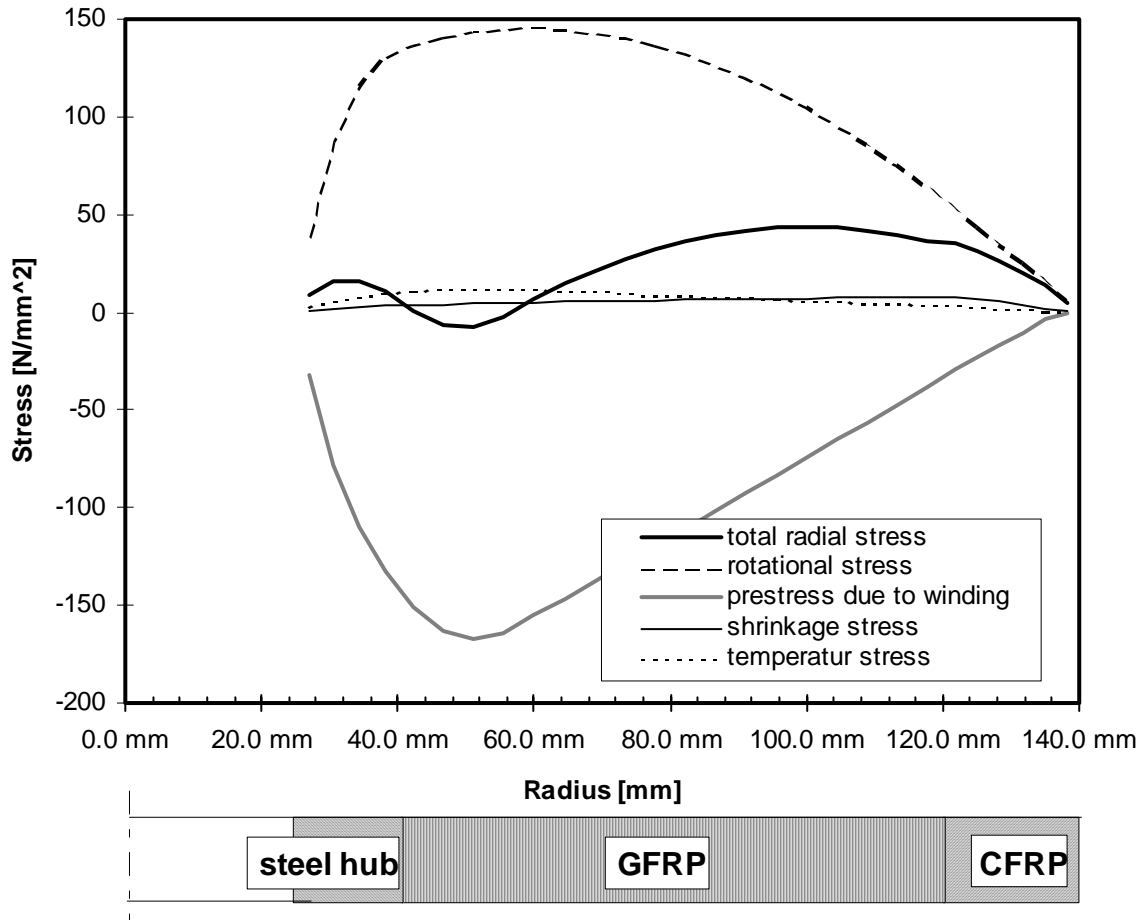


Figure 3: Radial Stress Distribution

MEASURED DATA

The predicted stresses or strains as calculated by the model above, have been compared with measured results. The result of these comparisons allows the verification of the model and gives an idea of the influence of each load.

MEASURING MANUFACTURING RELATED STRESS/STRAIN

A rotor with a diameter of 300 mm and a thickness of 45 mm served as test object. Together with the Swiss Federal Laboratories for Material Testing and Research (EMPA) some of the possible methods of measuring have been studied. Only manufacturing related stresses or strains have been measured, since the measurement of stresses or strains of high speed rotors is only possible with a large expenditure.

STRAIN GAUGE APPLIED TO SURFACE OF ROTOR

Initial measurements have been carried out on two geometrically identical rotors. One was wound without prestress and the second rotor with controlled prestress of about 10% of the ultimate tension of the glass fibre ribbon. Such prestressing results in a stress distribution as shown in Figure 4:

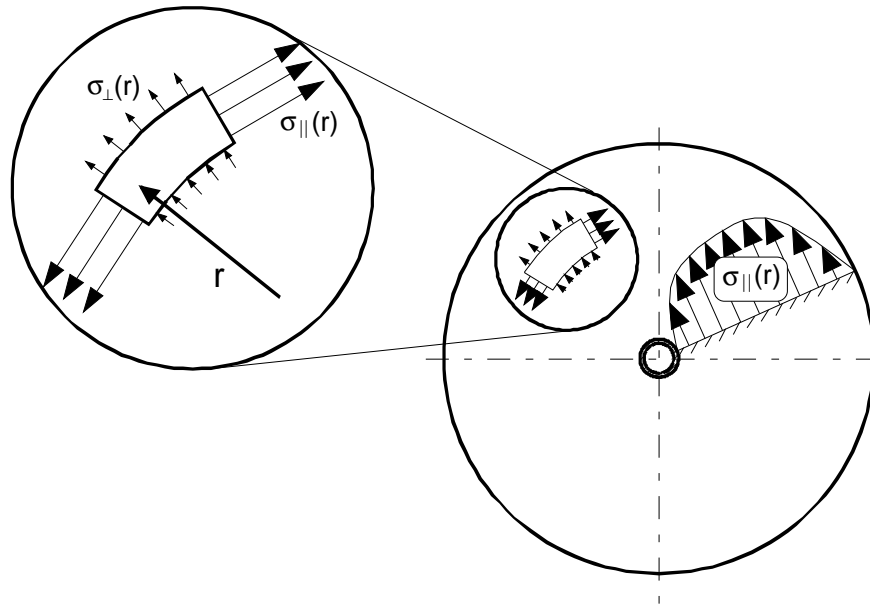


Figure 4: Stress Distribution in the Rotor

To minimize thermal stresses, the epoxy of the rotors has been cured at room temperature. At the upper and lower side of this disk-shaped rotor, strain gauges have been applied and the two rotors have been subsequently unwound. The unwinding of the fibre ribbon from the outside of the rotor frees the inner layers from the pretension load causing a variation in strain which are measured using the strain gauges.

OPTICAL MEASUREMENT OF DISPLACEMENTS

A similar unwinding test has been carried out with the Electronic Speckle Interference measuring method (ESPI). ESPI uses laser to illuminate an object to determine the interface of two subsequent images of the surface-structure. With this real-time method it is possible to monitor three dimensional displacements without disturbing the test object.

The gradient of displacement due to the subsequent unwinding is only in the order of μm per mm of unwound ribbon-material. The sensitivity of this method is dependent on the order of magnitude of the wave length of light and therefore sufficient to monitor these small displacements.

Figure 5 shows the results of the ESPI measurements. The measurements are fitted with the least square method. The figure shows the normalized function of the displacement per mm unwound ribbon-material to the actual radius. The measured data correspond well with the results of the calculation. The details of the measurement can be found in Hack, 1994.

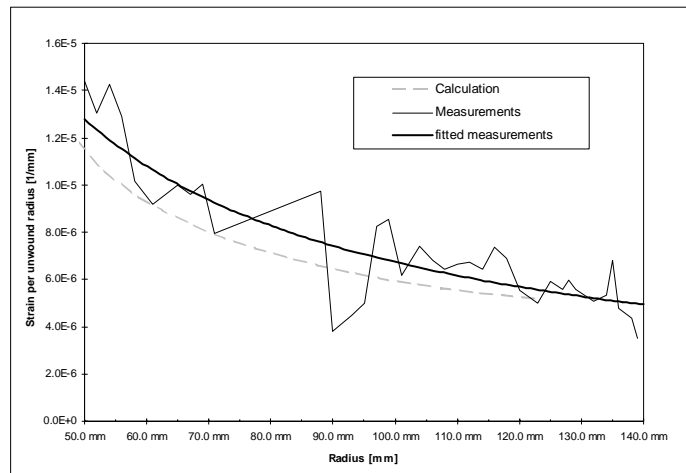


Figure 5: Measuring Results of the ESPI-Analysis

STRAIN GAUGE APPLIED DURING LAMINATION

The next idea was to manufacture a rotor with strain gauges inside the rotor. With this test set up it is possible to monitor all strains occurring during the manufacturing and curing of the rotor. To further separate the effects of the temperature load, a thermocouple has been jointly laminated into the composite.

Tests with strain gauges applied to unimpregnated ribbons have been carried out. The influence of bending, creep and fixation of the strain gauge as well as the temperature compensation have been evaluated in order to consider these effects in the calculation model.

Results of these tests have clearly demonstrated that the ribbon winding technology is sensitive to the pretension distribution of the ribbon which is not always constant, resulting in a reduction in the quality level.

CONCLUSIONS

The low ultimate radial strain is the limiting design factor of thick rim. Furthermore this type of rotor suffers from the influence of shrinkage and temperature strains. These

effects are difficult to handle and can lead to local overload of the material, resulting in cracks inside the rotors without applying rotational load.

The results obtained from these investigations show that thick rim flywheels benefit from the application of pretension.

With the developed finite element model has enabled the prediction of the stress/strain distribution of thick rim flywheels. The influence of pretension, shrinkage, temperature load and rotational load can be calculated and optimized. Practical laboratory tests showed good correlation with calculations.

REFERENCES

Dehnungsmessung an einem Schwungrad aus Glasfaserband mittels ESPI, E. Hack, EMPA Prüfbericht Nr. 147'682/1, 1994

Zur Erhöhung der Belastbarkeit von Bauteilen aus Faser-Kunststoff-Verbunden durch gezielt eingebrachte Eigenspannungen, H. Schürmann, Diss. GH Kassel, Vortschrittsberichte VDI, NR. 170, 1989

Woven ribbon composite flywheel with selfcentering hub, J. Widmer, IECEC, Florida 1985

Title: Stress Calculation Model for Thick Rim Flywheels

Author: Peter von Burg